# Determining the Conformations of Organic Macrocycles through a Combination of Dale's Rules, Molecular Mechanics, Solid-State $^{13}C$ NMR, and X-ray Diffraction

**Brian B. Masek, Bernard D. Santarsiero, and Dennis A. Dougherty*[1]**

*Contribution Number 7530 from the Arnold and Mabel Beckman Laboratories of Chemical Synthesis, California Institute of Technology, Pasadena, California 91125.*
*Received December 22, 1986*

**Abstract:** For the naphthalenophanes **C14**, **C15**, and **C16**, feasible ground-state conformations have been generated by using Dale's rules and the intrinsic conformational preferences of alkoxy naphthalenes. Molecular mechanics (MM) calculations were used to predict the most stable conformations. Solid-state, CP-MAS, $^{13}C$ NMR spectra have been interpreted by using Möller's relations between chemical shift and conformational sequence to validate the Dale/MM analysis. For C16, a complete structure determination by X-ray diffraction also confirms the conformational analysis.

Can one determine the ground-state conformation of an organic macrocycle without a crystal structure and without computationally evaluating perhaps thousands of potential minima? This is a fundamentally interesting question and one that has taken on increased significance with the discoveries of the ionophores[2] and macrolide antibiotics[3] and the continuing development of host–guest chemistry.[4] In the present work we show that for a series of large ring systems (20–22 atoms) that contain some structural constraints, a reasonable evaluation of the likely low energy conformations can be made with relatively little effort. The approach involves a combination of three methods: conformational analysis, as applied to macrocycles by Dale;[5] molecular mechanics (MM) calculations;[6] and Möller's analysis of polymethylene, solid state, $^{13}C$ NMR chemical shifts.[7] We have also used X-ray diffraction to substantiate arguments based on the other three techniques.

The molecules we have studied are the cyclophanes **1**, with $n$ = 14, 15, and 16, henceforth referred to as **C14**, **C15**, and **C16**. These are chiral molecules that can enantiomerize by a "jump rope" reaction, in which the aliphatic chain can loop around to the other face of the naphthalene. We have previously reported[8] a study of this dynamic process, which produced very intriguing results. For both **C14** and **C15**, $\Delta S^{\ddagger}$ for the enantiomerization was ca. −20 eu. This is a very large negative value for a unimolecular process in a hydrocarbon, which we took as an indication that the polymethylene chains of **C14** and **C15** are quite flexible in the ground states but quite restricted in the transition states. Remarkably, in **C16** this effect is completely absent ($\Delta S^{\ddagger}$ = −3 eu).

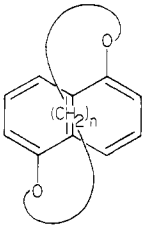


1

Part of the motivation for the present work was a desire to understand the substantial change in dynamic behavior on going from **C14** and **C15** to **C16**. We hoped that an understanding of the static stereochemistry, i.e., the ground-state conformations, would provide some insight into the dynamic stereochemistry. In addition, though, we recognized that these structures provide a good example of a common situation in modern organic chemistry. As alluded to above, macrocycles represent a quite important structural unit. In all applications of macrocycles, it is important to understand the shape of the molecule. The conformational properties of large ring alkanes ($(CH_2)_n$) can be quite complex but are fairly well understood.[9] However, most macrocycles of interest are not simple $(CH_2)_n$ molecules but generally contain substantial perturbations to the basic ring structure. These can make the problem still more complex or, as demonstrated below, can greatly simplify it. In the present case, the naphthalene system provides a well-defined structural subunit to the macrocycle. Starting with the conformational preferences of such a substructure and then applying simple principles from the conformational analysis of cycloalkanes, we have found that one can predict the preferred geometries of such a macrocyclic system.

## Conformational Analysis

In his pioneering work on the conformational analysis of medium and large ring alkanes, Dale arrived at two simple rules that are useful in constructing geometries for large rings.[5] For a ring to be formed, a certain number of gauche dihedral angles must be introduced. First, Dale found that a sequence of two gauche dihedral angles of the same sign was an efficient way to achieve chain bending. The energy cost of this deformation should be additive, i.e., twice the value of a single gauche interaction. This type of bend, which we shall call a normal corner, is found in unstrained diamond lattice type conformations of large rings.[10] Second, in even-membered rings, conformations with four normal corners, and therefore four sides, are found. For odd-membered rings it is impossible to fit together four sides so as to form normal corners, and three- or five-sided conformations are adopted.

We wished to test whether these principles could be extended to substituted or functionalized macrocyclic systems such as **1**, in order to predict low-energy conformations in these systems. By considering six atoms of the dioxanaphthalene system to be part of a macrocyclic ring (C1, C9, C10, C5, and both oxygens, see Figure 1), **C14**, **C15**, and **C16** are found to be 20-, 21-, and 22-membered rings, respectively. Thus, **C14** and **C16**, being even-membered macrocycles, would be predicted to adopt con-

(1) Camille and Henry Dreyfus Teacher-Scholar, 1984–1985.
(2) Dobler, M. *Ionophores and Their Structure*; Wiley: New York, 1981.
(3) For example: Gale, E. F., et al. *The Molecular Basis of Antibiotic Action*, 2nd ed.; Wiley: London, 1981.
(4) For an overview of the host–guest field, see: *Topics in Current Chemistry*: Vogtle, F., Ed.; Springer-Verlag: Berlin, 1981 and 1982; Vol. 98, 101, and 132 (1981, 1982 and 1986).
(5) Dale, J. *Acta Chem. Scand.* **1973**, *27*, 1115–1129.
(6) Burket, U.; Allinger, N. L. *Molecular Mechanics*; American Chemical Society: Washington, DC, 1982.
(7) Möller, M.; Gronski, W.; Cantow, H.; Höcker, H. *J. Am. Chem. Soc.* **1984**, *106*, 5093–5099.
(8) Chang, M. H.; Dougherty, D. A. *J. Am. Chem. Soc.* **1983**, *105*, 4102–4103. Chang, M. H.; Masek, B. B.; Dougherty, D. A. *J. Am. Chem. Soc.* **1985**, *107*, 1124–1133. See also ref 16.
(9) Dale, J. *Top. Stereochem.* **1976**, *9*, 199–270.
(10) Anet, F. A. L.; Cheng, A. K. *J. Am. Chem. Soc.* **1975**, *97*, 2420–2424.

0002-7863/87/1509-4373$01.50/0 

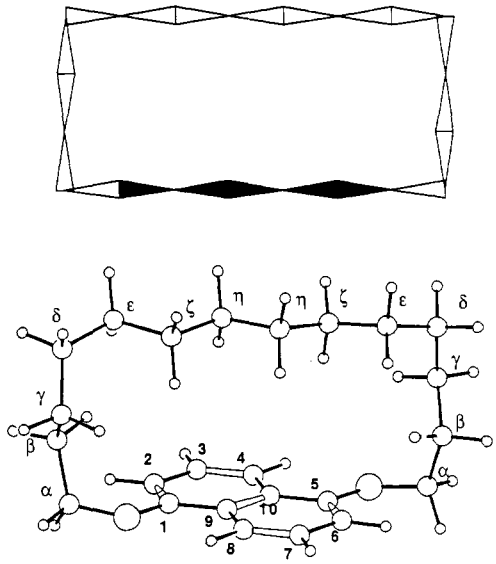

Figure 1. Dale projection (top) and MM2 geometry (bottom) of the [7373] conformation of **C14**. Filled wedges in the Dale projection are part of the dioxanaphthalene. Oxygen atoms are at the borders between the filled and open wedges.

formations with four normal corners, while **C15** might adopt conformations with either three or five corners. This assumes the dioxanaphthalene system is not too different from a polymethylene chain. The three bonds of the naphthalene ring (C1–C9, C9–C10, and C10–C5) are equivalent to three anti bonds in a cycloalkane, and thus they do not represent a major deviation from a conformation normally expected of a polymethylene chain.

The conformational preference of the aromatic ether functionality is also compatible with cycloalkane conformational preferences. Anisole prefers a planar geometry;[11] therefore, the first methylene of the cyclophanes (which we term $\alpha$) will prefer to lie in the plane of the naphthalene ring. The methylene will eclipse C2 of the naphthalene system, as opposed to C9 where it would encounter adverse nonbonded interactions with the peri hydrogen on C8. In this conformation, the naphthalene system and the $\alpha$ methylenes become equivalent to a sequence of five anti dihedral angles in a cycloalkane.

With the first methylene eclipsing C2, there are two conformations about the O–$CH_2$ bond, gauche or anti. However, the gauche conformer is destabilized by a nonbonded interaction with the hydrogen on C2 of the naphthalene ring, and so, one would predict a moderate preference for the anti conformation about this bond in the absence of ring constraints. In 1-ethoxynaphthalene, MM2 calculations predict the anti conformation to be preferred by 2.1 kcal/mol. Thus, in the absence of ring constraints, both the first and second methylenes have a preference to lie in the plane of the naphthalene ring. In this conformation, the naphthalene system plus the $\alpha$ and $\beta$ methylenes is equivalent to a sequence of seven anti dihedral angles in a cycloalkane and would give rise to a side nine bonds long according to Dale's rules.

Conformations of large rings are conveniently described with use of Dale's nomenclature.[5] Each "side" is defined as the region between two corners and assigned a number corresponding to the number of bonds between the corners. For example, Figure 1 shows a Dale projection[5] of the [7373] conformation of **C14** with a drawing of the MM2 geometry for this conformation. Both Dale projections and Dale's nomenclature will be used in this paper.

## Molecular Mechanics

Our previous work on these structures included a substantial number of MM calculations.[8] Our goal in that work was to enumerate, in a consistent, systematic way, possible low-energy conformations, because we wanted to evaluate any possible statistical contribution to $\Delta S^{\ddagger}$. We developed a special ring-making program to generate feasible structures, and indeed, we found literally thousands of viable conformations. In this work, we will try to rationally choose the best candidates for the global minimum for each structure and subject a minimal number of structures to a full MM evaluation. We have found that while the exhaustive (and exhausting) systematic approach did generate a number of low-energy structures, it did not uncover any minima that were lower in energy than those discussed below, nor did it uncover many of these structures. In the present work, geometry optimizations and energy evaluations were carried out with use of the MM2 force field[6,12] as implemented by the program BIGSTRN3.[13] Normal mode analysis ensured that all the structures discussed below are in fact minima on the potential energy surface.

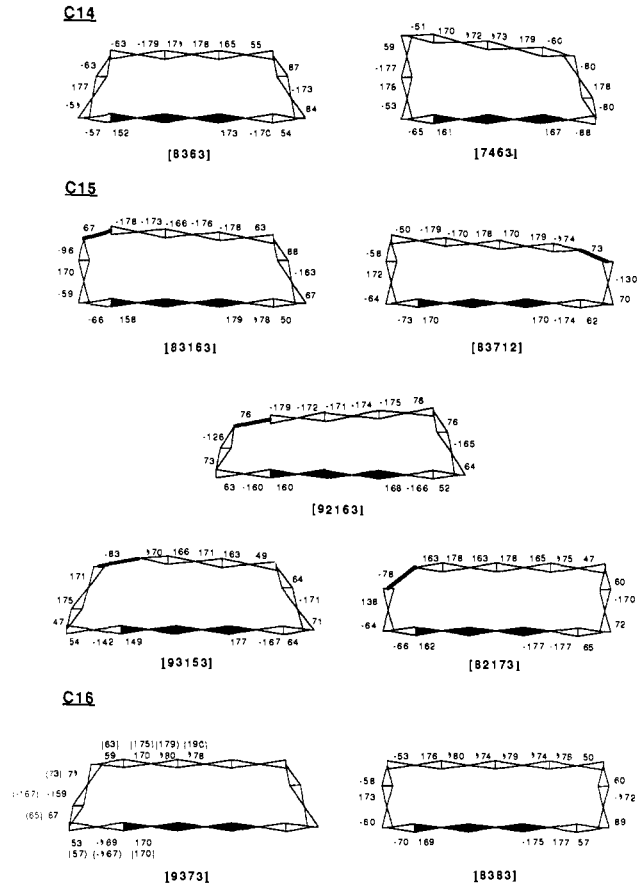


Figure 2. Dale projections of the low-energy conformations of **C14**, **C15**, and **C16**. Blackened bonds are part of the dioxanaphthalene. Oxygen atoms are at the borders between the filled and open wedges. Dihedral angles listed are MM2 (X-ray) values. For conformations with $C_2$ symmetry only half the angles are given.

**C14.** For cycloeicosane, Dale proposed [7373] and [6464] conformations as probable ground states.[14] For **C14**, along with these two conformations, one should consider the conformation with the first and second methylenes in the naphthalene plane, the [9353] conformation. However, in a 20-membered ring this leads to a large discrepancy between the lengths of the two opposite long sides, and this conformer would be expected to be of higher energy. A compromise would be the [8363] conformation which allows one $\beta$ and both $\alpha$ methylenes to be placed in their preferred positions. The results of MM2 calculations are shown in Table I. The [8363] conformation is found to be the ground state with the [7473] conformation 1.4 kcal/mol above it in energy. Dale projections of the two lowest energy conformations are shown in Figure 2.

(11) Anderson, G. M.; Kollman, P. A.; Domelsmith, L. N.; Houk, K. N. *J. Am. Chem. Soc.* **1979**, *101*, 2344–2352.

(12) Allinger, N. L. *J. Am. Chem. Soc.* **1977**, *99*, 8127–8134. Allinger, N. L.; Chang, S. H. M.; Glaser, D. H.; Hönig, H. *Isr. J. Chem.* **1980**, *20*, 51–56.

(13) Burgi, H. B.; Hounshell, W. D.; Nachbar, R. B.; Jr.; Mislow, K. *QCPE Bull.* **1986**, *6*, 96–97.

**Table I.** Low-Energy MM Conformations

| conformations | rel energy[a] | conformations | rel energy[a] |
|---|---|---|---|
| | **C14** | | |
| [8363][b] | 0.0 | non-Dale[b,c] | 3.2 |
| [7463] | 1.4 | non-Dale[b,c] | 3.5 |
| [7373] | 2.8 | [9353] | 4.3 |
| | | [6464] | 4.7 |
| | **C15** | | |
| [83163] | 0.0 | [966] | 2.8 |
| [83712] | 0.3 | [876] | 3.4 |
| [92163] | 1.2 | [867] | 4.1 |
| [82173] | 1.6 | [73443] | 4.4 |
| [93153] | 1.6 | [73434] | 5.0 |
| [83613] | 2.7 | [777] | 5.3 |
| non-Dale[b,c] | 2.8 | [74334] | 5.7 |
| | **C16** | | |
| [9373] | 0.0 | [8464][b] | 2.5 |
| [8383] | 0.6 | [9274][b] | 2.7 |
| [8473] | 1.6 | [7474] | 4.8 |
| [8374] | 2.3 | [6565] | 7.5 |

[a] kcal/mol. [b] Found by the systematic structure search. [c] Contains multiple single gauche sequences or other nonstandard corners.

**C15.** It is generally true that the conformational analysis of odd-membered rings is more complex than that of even-membered rings. For **C15** we considered more conformers than for **C14** and **C16**, beginning with those containing either three or five normal corners. Dale also states that five-sided conformations having a side one bond long are closely related to the quadrangular conformations of the even-membered rings immediately above or below in size.[5] Such conformations are derived from the conformations of the even-membered rings by insertion of one bond at a corner of the lower homologue or by cutting off a corner ring atom in the higher homologue. Such conformations have one "nonstandard" corner. A variety of standard trigonal, standard quinquangular, and ring expanded or contracted quinquangular conformations were considered. The results are shown in Table I. Dale projections of the low-energy conformations are shown in Figure 2. The lowest energy structure found, [83163], is derived from the [8363] conformation of **C14** by ring expansion, while the next lowest structure, [83712], is obtained by cutting a corner off the **C16** [8383] structure (see below).

**C16.** For cyclodocasane, Dale proposed three low-energy conformations, [8383], [7474], and [6565].[14] One might expect that for **C16** these would also be low-lying conformers. The trapezoidal [9373] conformation should also be considered as it allows the $\alpha$ and $\beta$ methylenes to be placed in their preferred positions. The results of the MM2 calculations are shown in Table I. The [9373] and [8383] conformations shown in Figure 2, are of nearly the same energy, with the other conformations at higher energies.

### X-ray Diffraction

As previously stated, cyclophanes **1** are chiral; they have at most $C_2$ symmetry. For all three compounds, the enantiomers are rapidly interconverting in solution at room temperature,[8] the temperature at which the crystals used for the X-ray diffraction studies were grown. It is interesting that all three compounds give crystals which belong to the chiral space group $P4_12_12$[15] with only one enantiomer present in a given crystal.

**C16.** The molecular structure of **C16** is presented in Figure 3. The conformation found in the crystal is [9373]. This conformation was predicted by MM2 to be the ground state *prior* to the crystallographic study. The molecule has $C_2$ symmetry, with the naphthalene planes lying perpendicular to crystallographic $C_2$ axes. These run along the *ab* diagonals and intersect both the C9–C10 and $C_\theta$–$C_\theta$ bonds at their midpoints. Dihedral angles are listed in Figure 2 along with the values from MM2 for comparison. It can be seen that MM2 values are in excellent agreement with experiment. Bond lengths and valence angles are provided as supplementary material. The experimental bond lengths are slightly short, presumably due to large amplitude motions in the crystal.

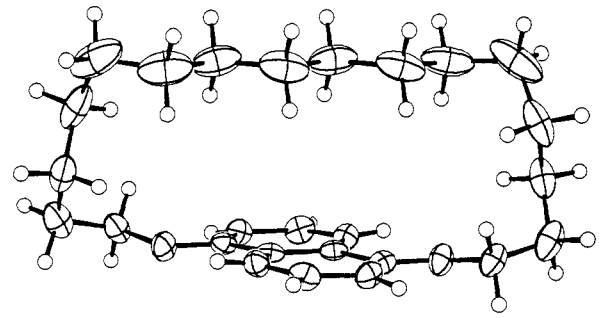

**Figure 3.** ORTEP drawing of the X-ray structure of **C16**. 20% probability ellipsoids are shown.

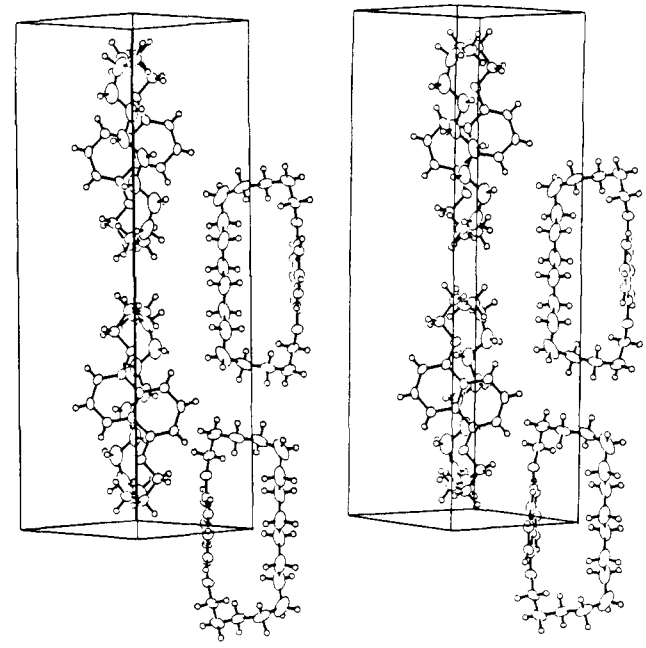

**Figure 4.** A stereoview of the molecular packing in the crystal for **C16**.

The crystal packing is illustrated in Figure 4. As can be seen from Figure 3, the molecule has a trapezoidal shape when viewed from the side. There is a crystallographic 2-fold screw axis coincident with the *c* axis which passes very near the midpoints of the $C_\gamma$–$C_\delta$ bonds. The molecule therefore packs along the *c* axis in columns with the short sides of the trapezoids abutting. Alternating molecules in the column are flipped by 180° about the *c* axis. The plane of the naphthalenes in the column is parallel to the (110) set of planes. There is a second such column, related to the $4_1$ axes at $x = {}^1/_2$ or $y = {}^1/_2$, that is coincident to the $2_1$ axis parallel to *c* which runs through the center of the unit cell. The planes of the naphthalenes in this second column are rotated by 90° with respect to the first column, i.e., they are parallel to the $(\bar{1}10)$ set of planes. The molecules in this column are displaced ${}^1/_4$ along the *c* axis (one-half the molecule's length along *c*) with respect to the first column.

**C14 and C15.** Although **C14** and **C15** crystallize in the same space group as **C16** and with very similar unit cell parameters (see Experimental Section), refined structures could not be determined, presumably due to disorder. Perhaps the first indication that these structures would be disordered came from parameters derived from the Wilson plots. The values obtained for an overall temperature factor, *B*, were 11.5 Å$^2$ for **C14** and 9.5 Å$^2$ for **C15**. In comparison, the value of *B* obtained from the Wilson plot for

(14) Dale, J. *J. Chem. Soc.* **1963**, 93.
(15) *International Tables for X-ray Crystallography*; Kynoch Press: Birmingham, England, 1974; Vol. IV.

**Table II.** Predicted Solid-State $^{13}C$ NMR Shifts in Polymethylene Chains[a]

| conformation | shifts (ppm) | conformation | shifts (ppm) |
|---|---|---|---|
| $G^{\pm}A{\cdot}G^{\pm}G^{\pm}$ | 23.6 | $AG^{\pm}{\cdot}G^{\pm}A$ | 28.7 |
| $G^{\pm}A{\cdot}AG^{\mp}$ | 25.0 | $AA{\cdot}AG^{\pm}$ | 30.4 |
| $G^{\pm}G^{\pm}{\cdot}AA$ | 27.9 | $AA{\cdot}AA$ | 35.5 |

[a] Möller, M., et al. *J. Am. Chem. Soc.* **1984**, *106*, 5093–99.

**C16** was 5.5 Å$^2$. All three data sets were collected for $1° \leq \Theta \leq 20°$ with Mo K$\alpha$ radiation.

As with **C16**, an attempt was made to solve the structures of **C14** and **C15** by direct methods. In each case, the naphthalene and the $\alpha$ carbon were positioned in the unit cell in the same position as for **C16**. The resulting Fourier maps[16] phased on these atoms revealed a continuous band or tube of electron density running ca. 4.0 Å above the naphthalene ring in roughly the positions of the carbon atoms along the chain for **C16**. However, disorder prevented the resolution of the positions of the carbon atoms along the chain and, therefore, full refinement of these structures was not possible.

Molecular mechanics calculations predict ground states with $C_1$ symmetry for both **C14** and **C15**. The lowest energy $C_2$ structures are 2.8 kcal/mol higher in both molecules. A $C_1$ structure that occupies the lattice site with twofold disorder would produce the observed crystallographic $C_2$ axis and would account for the disorder of the polymethylene chain. Such a disorder could be static or dynamic. If the disorder is due to the degenerate interconversion of a $C_1$ structure, giving rise to apparent $C_2$ symmetry (see Figure 8 for an example involving **C14**), then by cooling the crystal such motion might be frozen out and a full structure obtained. However, attempts to study **C14** at low temperatures were discontinued because the crystals fractured upon cooling.

Finally, it should be noted that **C14** could also be crystallized from ethanol to give orthothrombic crystals, space group *Pccn* ($a$ = 13.29 Å, $b$ = 10.12 Å, $c$ = 15.96 Å, $z$ = 4).[15] The naphthalene was found to lie perpendicular to a crystallographic $C_2$ axis, and the polymethylene chain was disordered.

### Solid-State CP–MAS $^{13}C$ NMR

We have shown that a Dale analysis produces relatively few potential ground state conformers for **C14–C16**, which can be easily evaluated by MM. For **C16**, X-ray crystallography confirms the ground-state prediction. For **C14** and **C15**, disorder prevented the determination of refined structures. It would be useful to have an easily applied experimental tool that could provide support for the Dale/MM predictions. This is especially true in situations where crystallography does not provide a complete answer. We were intrigued by the recent studies of Möller on the solid-state $^{13}C$ chemical shifts in polymethylene chains.[7] By studying cycloalkanes with both low-temperature X-ray diffraction and low-temperature CP–MAS $^{13}C$ NMR, it was found that the chemical shifts of the various carbons depended on the conformation about the two bonds on either side of a given methylene. The chemical shifts assigned to various conformational sequences are given in Table II. Two shifts are distinctive, being reasonably well separated from the rest and at each extreme upfield and downfield: the shift associated with the sequence AAAA at 35.5 ppm and the shift associated with $G^{\pm}AG^{\pm}G^{\pm}$ at 23.6 ppm. These could be especially useful tools for determining where the corners are in a molecule.

For a given conformation of **1**, the appearance of the solid-state $^{13}C$ NMR spectrum can be predicted on the basis of the results in Table II. For example, consider the [8363] conformation of **C14** (Figure 5). For the methylene labeled $\gamma$, the conformational sequence associated with the two bonds to either side is $G^+G^+AG^+$, which would be expected to give rise to a peak at 23.6 ppm. Likewise for the methylene labeled $\gamma'$ (which is *not* symmetry equivalent to $\gamma$), the conformational sequence is $G^-AG^-G^-$, and again a peak at 23.6 ppm is predicted. Note that in such spectra,

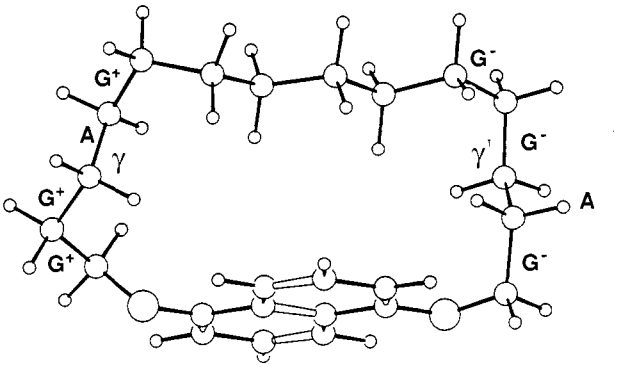


**Figure 5.** The [8363] conformation of **C14**.

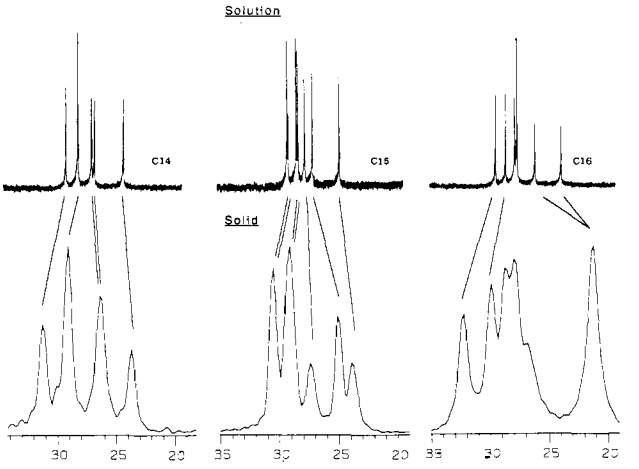


**Figure 6.** Aliphatic region of the $^1H$ decoupled $^{13}C$ NMR spectra in $CDCl_3$ solution (top) and CP–MAS $^{13}C$ spectra of the solid phase (bottom) of **C14**, **C15**, and **C16**.

peak intensities often accurately reflect atomic ratios. By studying a variety of organic compounds, Grant found that signal intensities agreeing with atomic ratios were obtained from $^{13}C$ CP–MAS spectra if a contact time of about 2.25 ms was used, and often with a contact time as short as 1.0 ms.[17] Möller also obtained quantitative spectra for cycloalkanes using a 3.0 ms contact time.[7] We used a 2.0 ms contact time. Because the carbons of interest are on the aliphatic chain and all have two directly attached protons, they should be cross polarized easily, and we can reasonably expect signal intensities to reflect atomic ratios.

Figure 6 shows the aliphatic region of both solid-state and solution $^{13}C$ NMR spectra for **C14**, **C15**, and **C16**. For all three compounds, crystals of the tetragonal lattice were used. In addition, for **C14** the orthothromic lattice was investigated, but the two spectra were identical, so our discussion will emphasize the tetragonal.

Because the $^1H$ NMR spectra have been previously assigned,[8] heteronuclear $^{13}C$–$^1H$ shift-correlated 2D NMR[18] allows complete assignment of the $^{13}C$ peaks in the solution spectra. All methylene groups for **C14** and **C16**, and all but the central methylene group for **C15**, consist of a diastereotopic pair of protons. Each pair is interconverted by the jump-rope reaction. For **C15** and **C16**, the jump-rope reaction is fast on the NMR time scale in solution, at room temperature.[8] Each $CH_2$ group produces only one signal in the $^1H$ NMR, and after consideration of the $C_2$ symmetry, eight aliphatic signals are expected. In the 2D NMR spectra of **C15** and **C16** (Figure 7) we have expanded the region containing the seven signals due to the $\beta$–$\theta$ methylenes. For **C14**, the jump-rope reaction is slow on the NMR time scale at room temperature,[8] and for the six methylenes $\beta$–$\eta$, 12 signals would be expected in

(16) Masek, B. B. Ph.D. Thesis, California Institute of Technology, 1987.

(17) Alemany, L. B.; Grant, D. M.; Pugmire, R. J.; Algers, T. D.; Zilm, K. W. *J. Am. Chem. Soc.* **1983**, *105*, 2133–2141, 2142–2147.

(18) *Two Dimensional Nuclear Magnetic Resonance in Liquids*; Bax, A., Ed.; Delft University Press: Holland, 1982.

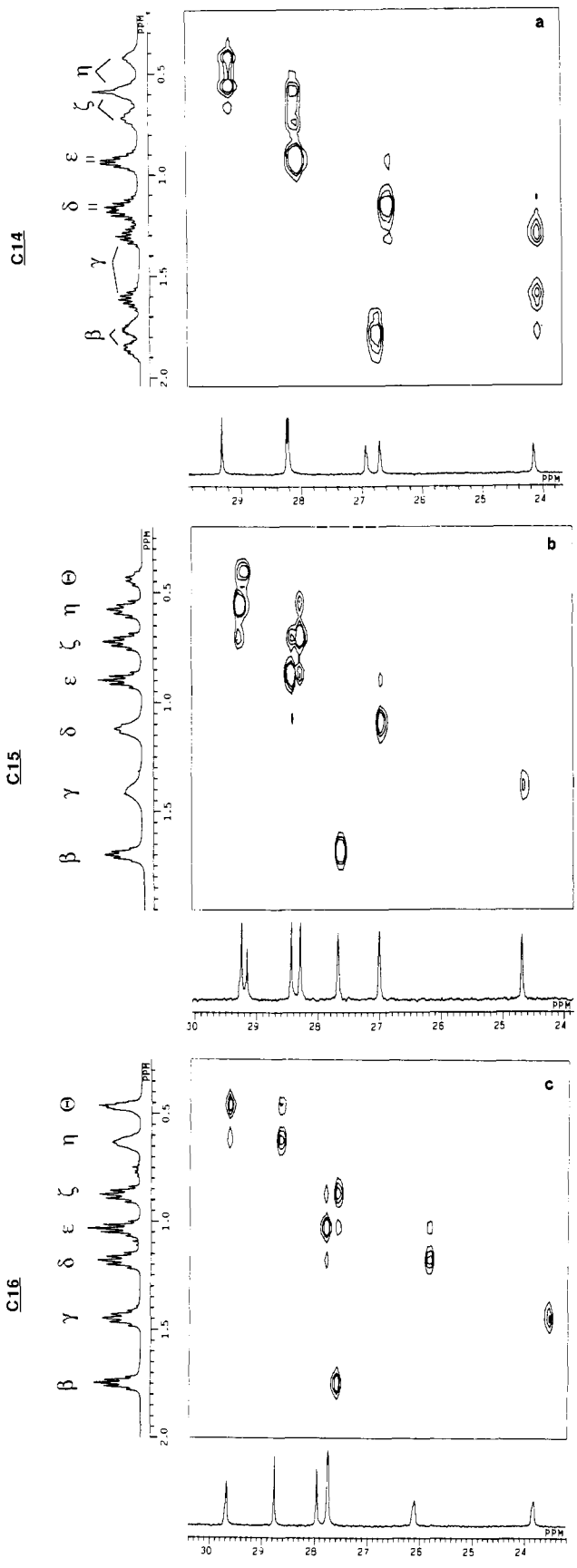


**Figure 7.** The aliphatic region of the heteronuclear $^{13}C$–$^{1}H$ shift-correlated 2D NMR of **C14**, **C15**, and **C16**.

the $^{1}H$ NMR. Two signals in the $^{1}H$ spectrum should correlate to each peak in the $^{13}C$ spectrum. Only eight $^{1}H$ signals are resolved, as can be seen from Figure 7. The two protons of the $\delta$ methylene have nearly the same chemical shift and therefore

**Table III.** Predicted and Observed $^{13}C$ NMR for **C14**

| | | | time av | | |
|---|---|---|---|---|---|
| carbon | solution[a] | solid | $C_2$-[8363] | $C_2$-[7463] | $C_2$-[3737] |
| $\alpha$ | 67.4 | 67.2 | | | |
| $\beta$ | 27.2 | 26.3 | | | |
| $\gamma$ | 24.4 | 23.7 | 23.6 | 24.2 | 23.6 |
| $\delta$ | 27.0 | 26.3 | 26.2 | 28.3 | 28.7 |
| $\epsilon$ | 28.5 | 29.1 | 28.3 | 28.3 | 27.9 |
| $\zeta$ | 28.5 | 29.1 | 29.2 | 29.2 | 30.4 |
| $\eta$ | 29.6 | 31.2 | 33.0 | 33.0 | 35.5 |
| rel energy[b] | | | 0.0 | 1.4 | 2.8 |

[a] $CDCl_3$. [b] kcal/mol.

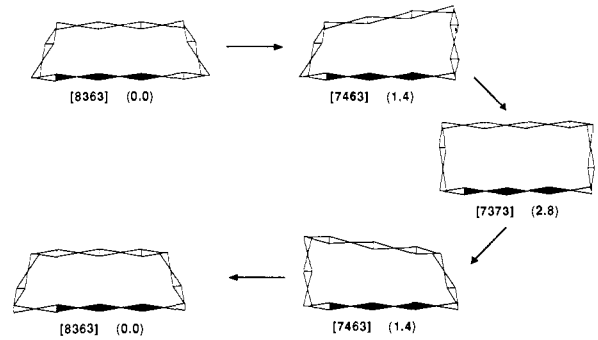


**Figure 8.** A pathway for the degenerate interconversion of the [8363] conformations of **C14**. Energies listed in parentheses are in kcal/mol relative to [8363].

a single multiple correlates to one peak in the $^{13}C$ NMR. The same is true for the $\epsilon$ methylene. Also, the signals due to the $\zeta$ and $\eta$ protons overlap, giving rise to three, not four, multiples. As can be seen in the 2D NMR, the peak at 0.58 ppm ($^{1}H$) correlates to two peaks in the $^{13}C$ spectrum and is due to a proton on each of these two methylenes.

The progression of the signals for the methylenes in the $^{1}H$ spectra, moving from left to right (downfield to upfield), is the same as the progression of the methylenes along the chain; i.e., the $\alpha$ protons are the most downfield, the $\beta$ protons are the next most downfield, etc.[8] This pattern is not carried over to the $^{13}C$ spectra. For all three compounds, it is the $\gamma$ carbon that gives the most upfield signal. The carbons in the center of the chain, $\eta$ and $\theta$, give the most downfield signal of the methylenes excluding $\alpha$.

**C14.** It is apparent from Figure 6 that the solution and solid-state spectra are quite similar. We can use this similarity to assign the peaks in the solid-state spectrum as shown. Deconvolution of the aliphatic region of the solid-state spectrum indicates that the peaks at 26.3 and 29.1 ppm have twice the area of the peaks at 23.7 and 31.2 ppm, consistent with the above assignments. The solid-state shifts assigned to the various carbons are listed in Table III along with the shifts predicted for the various low-energy conformations found by MM2.

The lowest energy conformation, [8363], with $C_1$ symmetry, is inconsistent with the $C_2$ symmetry indicated by solution $^{13}C$ and $^{1}H$ NMR and by the site symmetry in the crystals. However, rapid interconversion on the NMR time scale of the two equivalent [8363] forms would lead to "time averaged" $C_2$ symmetry. A potential pathway for this interconversion is outlined in Figure 8. The elementary step involved, $G^+G^+A$ changing to $AG^-G^-$, is a corner moving process that has been proposed to explain the dynamic behavior of other large ring compounds, both in solution[10,19,20,21] and in the solid state.[7] The barrier to such a corner move has been calculated for cyclododecane by MM and found

(19) Dale, J. *Acta Chem. Scand.* **1973**, *27*, 1130–1148.
(20) Anet, F. A. L.; Rawdah, T. N. *J. Am. Chem. Soc.* **1978**, *100*, 7166–7171.
(21) Anet, F. A. L.; Cheng, A. K.; Wagner, J. J. *J. Am. Chem. Soc.* **1972**, *94*, 9250–9252.

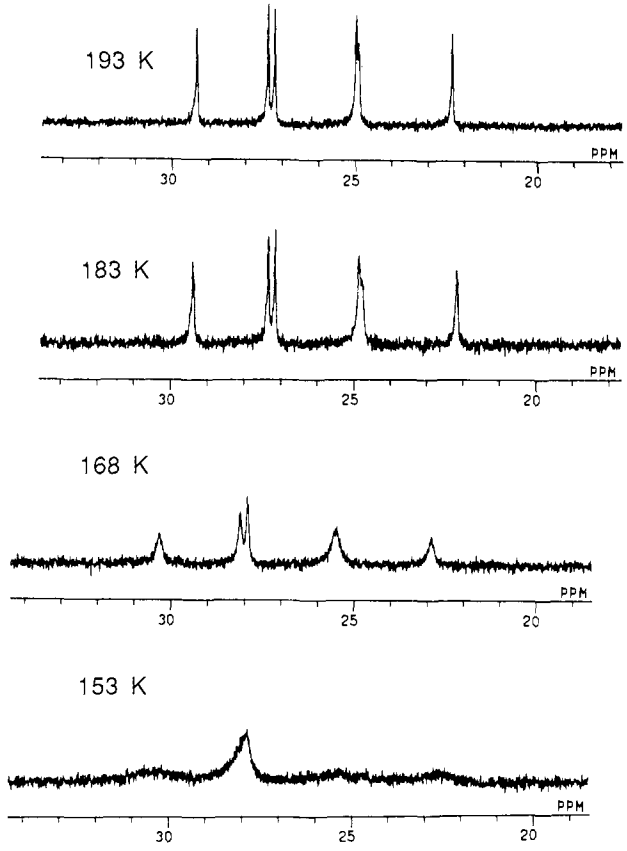


**Figure 9.** Variable temperature $^1H$ decoupled $^{13}C$ NMR solution spectra (aliphatic region) of **C14**.

to be 7.9 kcal/mol, in good agreement with the experimental free energy barrier of 7.3 kcal/mol in solution.[20] Möller has made the intriguing observation that the same process occurs in the solid state and with essentially the same barrier as in solution.[7] A time-averaged [8363] structure therefore seems quite feasible, and it is included in Table III. As can be seen, it best fits the observed shift data. Additional evidence implicating a dynamic structure for **C14** in solution is provided by $^{13}C$ NMR on cooling to 153 K (Figure 9). We know the broadening observed is due to chemical exchange because signals for the aromatic carbons remain sharp. If we take the coalescence temperature to be about 153 K and assume $\Delta\nu$, the frequency difference between the two coalescing peaks, to be about 3 ppm (300 Hz), then a crude estimate of 6.8 kcal/mol for the free energy of activation of the process causing exchange can be made.[22] This is similar to the barrier observed for corner moving in other systems.

**C15.** A comparison of the solution and solid-state NMR spectra again shows a great deal of similarity. This similarity was used to assign the peaks in the solid-state spectrum, as shown in Figure 6. Because there is only one $\theta$ carbon and two of every other ($\alpha$–$\eta$), the peak assignments should give rise to the ratio 1.5:2:1:1:1 for the areas of the aliphatic peaks (moving left to right (downfield to upfield)). Deconvolution of the aliphatic region gives the expected ratio. Because all of the predicted low-energy conformations have one nonstandard corner, and Möller studied only even-membered cycloalkanes having normal corners, it is not possible to make a quantitative prediction of the shifts for these conformations. However, qualitatively the trend is clear. As with **C14** and **C16** (vide infra), the $\gamma$ carbon is the most upfield at 23.9 ppm. This suggests a carbon in the sequence $G^{\pm}A{\cdot}G^{\pm}G^{\pm}$, putting the $\gamma$ carbon in a side three bonds long. More informative, the $\eta$ and $\theta$ carbons are the most downfield (as with **C14** and **C16**), indicating they are embedded in a sequence of anti dihedral angles (AA·AA). This rules out the regular trigonal and quinquangular conformations (e.g., [966], [876], [73443], etc.), which, because the naphthalene section is all anti, must have a corner near the middle of the polymethylene chains. Such shifts are only consistent with the ring expanded or contracted structures which are predicted to be of lower energy. So, while the solid-state $^{13}C$ chemical shift data does not allow the selection of a particular conformation, it does rule out several classes of conformations and is most consistent with the ring expanded or contracted structures, the structures predicted to be the low-energy conformations by MM2.

(22) At coalescence, the rate constant for the process causing exchange is given by $k = (\pi\Delta\nu)/2^{1/2}$. See: Sandström, J. *Dynamic NMR Spectroscopy*; Academic Press: New York, 1982.

**Table IV.** Predicted and Observed $^{13}C$ NMR for **C16**

| carbon | solution[a] | solid | $C_2$- [9373] | time av $C_2$- [8383] |
|---|---|---|---|---|
| $\alpha$ | 66.7 | 65.9 | | |
| $\beta$ | 28.0 | 27.2, 28.3, or 29.0 | | |
| $\gamma$ | 24.0 | 21.6 | 23.6 | 23.6 |
| $\delta$ | 26.3 | 21.6 | 23.6 | 26.2 |
| $\epsilon$ | 28.2 | 27.2, 28.3, or 29.0 | 28.7 | 28.3 |
| $\zeta$ | 28.0 | 27.2, 28.3, or 29.0 | 27.9 | 29.2 |
| $\eta$ | 29.0 | 30.2 | 30.4 | 33.0 |
| $\theta$ | 29.9 | 32.6 | 35.5 | 35.5 |
| rel energy[b] | | | 0.0 | 0.6 |

[a] $CDCl_3$. [b] kcal/mol.

**C16.** As can be seen from Figure 6, a comparison of the solution and solid-state NMR spectra again shows some similarity. In the solution spectrum, a peak at 28.0 ppm can be seen by heteronuclear $^{13}C$–$^1H$ correlated 2D NMR to be a coincidence of 2 peaks, the peaks for the $\beta$ and $\zeta$ carbons (Figure 7). However, deconvolution of the solid-state spectrum indicates that it is the peak at 21.6 ppm in the solid which is the double peak. Of the two low-energy conformations found by MM2, only one, the [9373] conformation, would be predicted to have a double intensity peak for the most upfield peak (see Table IV). As already stated, single-crystal X-ray diffraction shows the conformation to be [9373]. On the basis of analogy to the solution spectrum, the two most downfield aliphatic peaks of the solid-state spectrum can also be assigned, as shown in Figure 6. It is difficult to assign the middle three peaks to particular carbons, as the shifts are so close to each other. Any assignment of these peaks would result in a satisfactory agreement between both solution and solid spectra and between the solid-state spectrum and that predicted for the [9373] conformation.

The differences between the solid-state and solution NMR spectra may be due to the presence of a second conformation in solution. MM2 calculations predict the [8383] conformation is 0.6 kcal/mol higher in enthalpy than [9373]. However, because [8363] is of lower symmetry ($C_1$) than [9373] ($C_2$), the former will be favored by an entropic factor of $R$ ln 2 or ca. 0.4 kcal/mol at room temperature. Thus, the two conformations are likely to be very close in energy, and both may be significantly populated at room temperature. Interconversion by a corner moving process would be expected to occur very rapidly on the NMR time scale, and thus an averaged spectrum is observed in solution. This would lead to a downfield shift of the $\delta$ carbon in solution, as is observed.

## Discussion

We will first summarize our findings. Starting with the constraints enforced by the naphthalene, adding the conformational preferences of aryl ethers, and then applying Dale's simple analysis leads to relatively few probable conformers. For **C16** MM predicts two low-energy structures, [9373] and [8383]. The solid-state $^{13}C$ NMR spectrum contains an upfield signal of double intensity consistent only with that of [9373]. This assignment is confirmed by the X-ray structure. The solution $^{13}C$ NMR differs from that in the solid state in a way that is fully consistent with a rapid equilibrium between the two low-energy conformations. For the odd-membered ring **C15**, the lowest lying structures are predicted to belong to the ring-expanded or ring-contracted types of con-

formations. This prediction is strongly supported by the NMR data, although it is not possible to identify the particular ground-state conformation. For **C14**, the [8363] conformation is predicted to be the ground state, and the solid-state NMR data support this conclusion.

For both **C14** and **C15**, the ground states have $C_1$ symmetry. However, solution $^1H$ and $^{13}C$ NMR, solid-state $^{13}C$ NMR, and X-ray diffraction indicate $C_2$ symmetry. A rapid interconversion in both solution and solid, giving rise to "time-averaged" $C_2$ symmetry, is proposed. This is supported by variable temperature solution $^{13}C$ NMR for **C14** and is consistent with the disorder observed by X-ray diffraction for both **C14** and **C15**.

We note that all three molecules share common features. The ordering of the signals in the $^1H$ NMR spectra is the same for all three compounds.[8] In the $^{13}C$ NMR spectra, the $\gamma$ carbons always give the most upfield signals, and the central carbons ($\eta$ and $\theta$) always give the most downfield signals. The predicted conformations all have a basically rectangular shape, with two long and two short sides. In all the conformations, the $\gamma$ carbons reside in the short sides with one proton pointed in at the naphthalene, with its ring currents, and the other proton pointed out away. This explains why, for all three compounds, the $\gamma$ protons consistently show a large chemical shift difference.[8] Similarly, the carbons in the center of the chains of all three compounds form a zigzag parallel to the plane of the naphthalene, and this points one proton down at the naphthalene and one up and away. Again large chemical shift separations are observed for the central methylenes.[8] The $^{13}C$ shifts of these carbons may also indicate some shielding by the naphthalene since in each case they are upfield of the 35.5 ppm predicted by Möller for a AAAA sequence.

Overall, these results are quite encouraging. There is complete consistency among the data and the MM predictions. It is remarkable that the simple Dale/MM analysis can produce the correct conformations of such large flexible molecules. For the cyclophanes **1**, solid-state CP–MAS $^{13}C$ NMR was successful in providing useful information unavailable by X-ray diffraction. The shifts determined by Möller[7] provide a tool which should prove valuable in studies of other molecules containing polymethylene chains. It would appear that large-ring conformational analysis is not unmanageable if there is a structural element that provides some measure of order.

## Experimental Section

**General.** The preparation of **C14**, **C15**, and **C16** has been described elsewhere.[8] Routine $^1H$ and $^{13}C$ NMR spectra and the 2D NMR spectra were taken on a JEOL-GX400 spectrometer.

**X-ray Diffraction.** Crystals of all three cyclophanes were grown from acetonitrile and are transparent, multifaceted prisms. For both **C14** and **C16**, oscillation photographs and zero-level and first-level Weissenberg photographs were taken as part of a preliminary investigation to determine the space group and unit cell parameters. It was evident from the photographic workup that the crystals were tetragonal and were mounted along the $c$ axis, which was typically the long axis of the crystal. The intensity data indicated the following systematic absences: 001 absent for $l \neq 4n$, $h00$ and $0k0$ absent for $h$ or $k$ odd, consistent with the space group $P4_12_12$ (No. 92).[15] The cell constants are $a = b = 9.168$ (4), 9.143 (2), 9.126 (5) Å; $c = 26.23$ (2), 27.254 (5), 28.071 (9) Å; $Z = 4$; for **C14**, **C15**, and **C16**, respectively. They were determined by least-squares refinement of the setting angels of 25 reflections in the range $13° < 2\theta < 22°$ for **C14**, $10° < 2\theta < 26°$ for **C15**, and $10° < 2\theta < 16°$ for **C16**. The intensity data for all three compounds were collected on an Enraf-Nonius CAD4 diffractometer with a graphite monochrometer and Mo K$\alpha$ radiation ($\lambda = 0.7107$ Å), $2° \leq 2\theta \leq 40°$. A scan rate of ~1 deg/min for $\omega$ scans was used. For **C14**, a hemisphere ($\pm h,+k,\pm l$) of data was collected (4578 reflections). For **C15**, all but one quadrant ($\pm h,-k,-l$) of data were collected (7787 reflections). For **C16**, one full quadrant ($+h,+k,\pm l$) plus part of an additional quadrant ($+h,-k,\pm l$) of data were collected (4657 reflections). During data collections, three standard reflections were remeasured after every 5000 and showed no unusual deviation in intensity. The data were averaged over $4/mmm$ symmetry to give 666, 689, and 717 reflections for **C14**, **C15**, and **C16**, respectively. The crystals used for data collection wre 0.43 × 0.43 × 0.43 mm in size for **C14**, 0.36 × 0.36 × 0.36 mm for **C15**, and of similar size for **C16**.

The structure of **C16** was solved in the lower symmetry space group $P4_1$ by direct methods with the program MULTAN.[23] This yielded the coordinates of the naphthalene group, the oxygen atoms, and twelve of the carbon atoms in the polymethylene chain. The positions of the remaining four carbons were determined by subsequent phasing and Fourier synthesis. Full-matrix least-squares refinement on $F^2$ was carried out in the higher symmetry space group $P4_12_12$, minimizing the function

$$\sum\omega[F_o^2 - (F_c/k)^2]^2$$

The asymmetric unit contains half of the molecule, with the other half related by a $C_2$ rotation. The scale factor, the coordinates and anisotropic Gaussian parameters of the carbon and oxygen atoms, plus the coordinates and isotropic Gaussian parameters of the hydrogen atoms of the naphthalene were included in the refinement, giving a total of 139 parameters. The hydrogen atoms on the carbon atoms of the polymethylene chain were not refined but were simply placed in calculated positions. The scattering factors were taken from ref 15. The final cycle yielded a goodness-of-fit

$$S = \{\sum\omega[F_o^2 - (F_c/k)^2]^2/(n - v)\}^{1/2}$$

of 2.3 for 717 reflections; $R = \sum||F_o| - |F_c||/\sum|F_o| = 0.075$ ($I_{obsd} > 0$, $n = 676$) and $R' = 0.054$ ($I_{obsd} > 3\sigma$, $n = 491$). The final values of the parameters are provided as supplementary material along with the structure factor amplitudes. All calculations were carried out on a VAX 11/750 computer with MULTAN[23] and the CRYRM[24] system of programs.

**CP–MAS $^{13}C$ NMR.** The NMR data were obtained on a home-built spectrometer operating at a carbon frequency of 50.4 MHz and equipped with a CP–MAS probe from Doty Scientific with 7 mm o.d. sapphire rotors. The samples were generally spun at speeds of 3.2–4.2 kHz. The $^1H$ 90° pulse length was usually 5 $\mu$s. Cross-polarization contact times were 2.0 ms, and the Hartmann–Hahn matching condition was set with use of an adamantane standard, whose methylene peak also furnished a chemical shift reference at 38.56 ppm from $Me_4Si$.[25] The cross-polarization pulse program incorporated spin-temperature inversion[26] to suppress artifacts, and "flipback" of the $^1H$ magnetization to decrease the recycle delay. A "rolling base line" in some spectra was eliminated by left-shifting the free-induction decay and by using a base line fit routine on the Nicolet 1280 computer. Deconvolution of peak intensities was carried out with use of the Nicolet NMC software.

**Acknowledgment.** Solid-state NMR was done at the NSF Southern California Regional NMR facility. We thank Dr. Dick Marsh, Dr. Bill Schaefer, and Doug Meinhart for helpful discussions.

**Registry No. 1** ($n = 14$), 94427-68-6; **1** ($n = 15$), 85851-49-6; **1** ($n = 16$), 94427-69-7.

**Supplementary Material Available:** Details of the X-ray structure of **C16**, including Atom Coordinates and $U_{eq}$ (Table V), Anisotropic Gaussian Parameters (Table VI), H Atom Coordinates and $B$'s (Table VII), Bond Lengths (Table VIII), and Valence Angles (Table IX) (5 pages); and structure factor amplitudes (Table X) (3 pages). Ordering information is given on any current masthead page.

(23) Germain, G.; Main, P.; Woolfson, M. M. *Acta Crystallogr., Sect. A* **1971**, *A27*, 368–376.
(24) Duchamp, D. J.; Trus, B. L.; Westphal, B. J. (1964) CRYRM Crystallographic Computing System. California Institute of Technology, Pasadena, CA.
(25) Earl, W. L.; Vanderhart, D. L. *J. Magn. Reson.* **1982**, *48*, 35–54.
(26) Stejskal, E. O.; Schaefer, J. *J. Magn. Reson.* **1975**, *18*, 560–563.